"A"

57/72

# The Experimental Identification of Individual Particles by the Observation of Transition Radiation in the X - Ray Region

F. Harris, T. Katsura, S. Parker and V.Z. Peterson,
University of Hawaii.

R.W. Ellsworth and G.B. Yodh,
University of Maryland.

W.W.M. Allison, C.B. Brooks, J.H. Cobb and J.H. Mulvey,
Oxford University.

## 1. Introduction

The phenomenon of transition radiation, first predicted by Ginzberg and Frank[1] has been explored extensively by Russian groups[2-5] and also by Yuan and his collaborators at Brookhaven[6-9]. Our intention in the experiment to be described in this report was to study the possibility of using this effect to identify efficiently individual particles of very high $\gamma$ (i.e. $\gamma = E/m > 1{,}000$). The results[10] confirm the predictions of others [2, 4, 9, 11] that individual particles can be identified. The experiment was conducted at the Bevatron in December 1971 using two sets of foil radiators and one set of styrofoam radiators (see paragraph 2.2). We defer comparison with theoretical predictions of transition radiation yield to a later report, following a more comprehensive series of experiments which will be performed at SLAC this summer. A good review of the theoretical basis is given by Garibian[5].

## 2. The Experiment

### 2.1. Method

The method is to detect the x-rays emitted when a charged particle traverses an interface separating two media of different refractive index, in this case mylar-air. Since the probability of emission is $\sim \alpha$ per interface the effect must be amplified by the use of many interfaces, such as a series of mylar foils. This is made possible by the fact that the x-rays are highly collimated along the particle trajectory, the typical emission angle being $\sim 1/\gamma$.

However, absorption of the x-rays in the foils limits the number of foils that can be effective. In addition, interference between the radiation emitted at the two foil surfaces results in a yield which decreases proportionally to $t^2$ when t (the foil thickness) falls below $t_f$ the "formation zone"[5] for the foil material[12].

The compromise between primary yield and absorption leads to an arrangement in which a series of radiators (each consisting of about 100 foils) are interleaved with x-ray detectors (see figure 1). A multiwire proportional chamber (MWPC) is an excellent detector of transition-radiation, especially if filled with a high Z gas such as Krypton or Xenon: the efficiency is good for x-rays in the 3-20 KeV region, the ionization loss by the charged particle is low, the angular acceptance is high and if necessary several contemporaneous particles can be spatially resolved

and so separately identified (by virtue of the $1/\gamma$ emission angle the transition radiation photons remain close to the parent particle trajectory.)

## 2.2. Apparatus.

In this experiment we used 11 MWPC each preceded by radiator stacks containing 100 mylar foils. Two radiator configurations were used: foil thickness, t = 1/6 mil[13] and air-spacing, d = 60 mil; t = ½ mil with d = 30 mil.

The chambers had a sensitive volume of 20 cm x 20 cm x 1.5 cm and their construction has been described by S. Parker et al[14]. For this experiment all the signal-wires were strapped together and one pulse height recorded for each chamber. Two gas fillings were used: 93% Argon + 7% Methane and 93% Krypton[15] + 7% Methane. The chamber windows were ¼ mil aluminized mylar.

Data were taken at two values of beam momentum: 1.3 GeV/c and 3 GeV/c. The experimental layout is shown in figure 1. In addition to three beam defining scintillation counters, three Cerenkov counters and a lead-lucite shower counter were used to identify the small percentage of electrons in the negatively charged beam (∿0.2% at 3 GeV/c and ∿2.2% at 1.3 GeV/c). The $\pi^-$ - meson contamination of 3 GeV electron triggers was measured to be much less than 1%.

The effect of bremsstrahlung and $\delta$-rays produced in the foils was estimated to be negligible. However, to determine background from such processes runs were made in which the radiators were replaced with single sheets of plastic of the same total thickness and also others with no material present.

The charge from each chamber was readout with a preamplifier and sample-and-hold. All eleven chamber signals and the shower counter pulse height were displayed on a CRT to be recorded on 35mm film. In addition the signal from chamber 1, delayed by 200 nsec, was taken direct to the CRT and also displayed so that in the analysis stage all events in which another particle had traversed the system within the integration time of the sample-and-hold (∿3μ sec) could be excluded. On average ∿ 12% of recorded events were rejected for this reason; the time distribution of double-pulses indicates that in the worst case less than 4% of the remaining events were unresolved two particle events.

All the data recorded on film was measured by the Oxford PEPR[16], about 80,000 frames in 36 hours.

## 2.3. Energy Calibration

At frequent intervals during the runs each chamber was exposed to an $Fe^{55}$ x-ray source (5.9 KeV) and calibration data recorded, also on film.

These measurements showed a systematic variation of the chamber gains with time; all chambers followed the same pattern which had a full excursion of $\sim$ 20% over the 24 hours in which most of the data was taken. This effect was probably due to pressure and temperature changes. The $Fe^{55}$ data were used to correct for this chamber-independent variation.

In the normal (data taking) mode of readout the trigger was provided by the beam particle selection logic; the $Fe^{55}$ x-rays on the other hand had to be self-triggered. When measurements were made taking the output of a single chamber preamplifier directly to a pulse-height-analyser, a different relative pulse-height from $Fe^{55}$ x-rays and the peak of the 3 GeV/c $\pi^-$ ionization loss distribution was obtained. We attribute the difference observed between the two modes to a systematic loss suffered by the signal from $Fe^{55}$ x-rays in the self-triggered normal readout due to delays in the trigger circuit. Consequently we have chosen the $Fe^{55}$ and 3 GeV/c $\pi^-$ data taken with the direct readout to a pulse height analyser as the basis of our absolute energy calibration; however we must assign an uncertainty of at most 20% to this calibration procedure.

Although the linearity of chamber response was established beyond the range of interest the readout system (including CRT display) introduced a saturation effect which was not the same in magnetude for all chambers. The saturation level varied between 11.5 KeV and 21 KeV; in figures showing distributions of chamber pulse height all data above the lowest saturation level are shown in one overflow bin.

## 3. Results

### 3.1 The Distribution of Ionization Loss and the Relativistic Rise

We show in figure 2 A the distribution of ionization loss by 3 GeV/c $\pi^-$ - mesons in a single Argon + Methane filled chamber (data taken without radiators); figure 2B shows the distribution obtained when the signals from 11 chambers are summed. The curves are the predictions of Blunck and Leisegang [17]. As observed by others [18, 19, 20] the experimental distribution is narrower than the Blunck-Leisegang theory for the single chamber, but agreement is reasonable for the "sum of 11" if the system is treated as a single chamber of thickness 11 x 1.5 cms [21]. Figures 3A and 3B show the same distributions for 3 GeV/c electrons. Our widths (FWHM) agree well with the data of West [22].

The data show the presence of the relativistic rise. Figure 4 shows our measurements of the relative most-probable energy loss, for both $\pi^-$ - mesons and electrons, in a single chamber filled with Argon + Methane and also Krypton

+ Methane. The curves are predictions from Sternheimer and Peierls[23] and the data are normalised to them at the 3 GeV/c $\pi^-$ points (there is no density-effect correction for $\pi^-$ - meson momenta below $\sim$ 14 GeV/c). For 3 GeV/c $\pi^-$ - mesons ($\gamma$ = 21.6) the Sternheimer and Peierls prediction of most-probable energy loss per chamber with Argon + Methane filling is 2.3 KeV compared with our measured value of (2.2 $\pm$ 0.1) KeV; the corresponding figures for Krypton + Methane are 4.3 KeV and (4.2 $\pm$ 0.2) KeV. But these values are subject to an uncertainty in energy calibration of up to 20% (see paragraph 2.3). Other data are given in Table I; in agreement with other experiments[20] these results suggest that the plateau reached by the ionization loss at large $\gamma$ is not as high as is predicted by Sternheimer and Peierls.

### 3.2 Transition Radiation

When 3 GeV/c electrons pass through the system with the ½ mil. mylar radiators in place the single chamber pulse-height distribution obtained is the histogram shown in figure 5A. By comparison with figure 3A, obtained without radiators (actually equivalent absorber and no absorber data combined), it is clear that there is an additional source of energy deposition; this we ascribe to transition radiation.

The with and without-radiator distributions can be compared quantitatively in the following way. Self-absorption in the foils effectively removes all photons of less than 3 KeV, also in Argon there are few examples of ionization loss less than 1 keV per chamber; therefore almost none of the pulses less than 4 keV should be associated with a transition radiation photon - this part of the distribution is 'pure' ionization energy loss. So we can match the shapes of the no-radiator and with-radiator distributions below 4 keV; this has been done by normalising to the same number of events in the 1 → 3 keV interval. The result is the shape marked by dots superposed on the histogram of figure 5A; this then also shows the number of 'pure' ionization loss signals above 3 keV. In fact the ionization-loss shape follows the histogram well up to about 4.5 keV, confirming that there are very few photons of energy less than $\sim$3 keV, entering the chambers.

As the average number of transition radiation photons detected in each chamber is less than one we can estimate a lower limit to the number of detected photons, $N_\gamma$, from the number of pulses in excess of the ionization-loss shape. The result is 3.6 $\pm$ 0.7 summed over all 11 chambers per incident electron; the error is mainly due to systematic effects, such as relative calibrations, but is not affected by the energy saturation in the readout system. Figure 5B shows the data for Krypton filling with its greater efficiency for photon

detection; in this case $N_\gamma = 5 \pm 0.5$.

The figures for $N_\gamma$ and also total energy deposition for different radiator configurations and momenta are summarised in Table II. The effect of saturation is that the mean energies given in Table II are systematically low. Using information from the channels with highest saturation and assuming a linear fall off above the saturation point, an estimate of the error has been made; this varies from 2-3% for the π-meson data to a shift in the mean of about 10% for the electron data in Krypton with ½ mil. radiators.

Table II includes two sets of data, rows 1 and 6, for which no transition radiation effect should be observed. Row 1 is for 3 GeV/c mesons passing through the ½ mil. radiators and row 6 gives data for 3 GeV/c electrons passing through equivalent absorbers consisting of single sheets of plastic 50 mil. thick. In neither case is a significant effect observed. The values of $N_\gamma$ and energy deposited by transition-radiation photons for 1 and 6 can be taken as indicating the uncertainties in the determination of these quantities. This perhaps suggests that the assigned errors, which are based on an estimated 5% uncertainty in relative calibration of runs made at different times, are conservative.

The yield from 1/6 mil. foils is significantly lower than that for ½ mil. foils. This thickness dependence, already observed by Yuan, et al[7], is related to the coherence between the radiation from the leading and trailing interfaces of the foil and the observed drop in yield is in reasonable agreement with that expected when the thickness falls below the value of the formation zone.

The one run (row 8, Table II) made with slabs of 2" thick Styrofoam as radiators confirms earlier reports[2,9] that transition radiation is generated in this material; in this case the yield was about half that obtained with 100 ½ mil. mylar foils as radiator.

Row 7 in Table II gives results obtained when the ½ mil. foils were tilted at an angle of 30° to the incident 3 GeV/c electron beam. The result is close to that obtained for normal incidence (row 3).

Figure 6 shows three distributions of the sum of pulse heights from all eleven chambers filled with Argon + Methane. On the left is that for 3 GeV/c $\pi^-$ - mesons, on the right and shaded is that for 3 GeV/c electrons passing through the ½ mil. radiators and the one in the middle is for 3 GeV/c electrons without radiators. The difference between $\pi^-$ - mesons and electrons (no radiators) due to the relativistic rise is clear, as also is the upward shift of the electron with radiators distribution due to transition radiation.

Figure 7 shows the corresponding distributions for Krypton + Methane in the chambers. These are a further demonstration of the greater efficiency of Krypton for the detection of photons, associated with the K absorption edge

at 14.3 keV. The results show a significant relative displacement of the distributions for electrons with, and without radiators and suggest that particle identification is possible by the detection of transition-radiation in the presence of ionization loss.

ACKNOWLEDGEMENTS

The authors are grateful to Dr. J.G. Løken for writing the programme to measure the film on the Oxford PEPR. They also wish to thank the staff of the Bevatron and Lawrence Berkeley Laboratory for their aid and hospitality. Dr. M.L. Stevenson is thanked for his assistance in the early stages of the experiment. Several discussions with members of the Brookhaven group working on transition radiation have been very useful.

The A.E.C. (Hawaii), N.S.F. (Maryland) and the R.H.E.L. (Oxford) are thanked for financial support.

## REFERENCES AND FOOTNOTES


1. V.L. Ginzberg and I.M. Frank, JETP 16 15 (1946)
2. A.I. Alikanian, K.M. Avakina, G.M. Garibian, M.P. Lorikian and K.K. Shikhliarov, P.R.L. 25 635 (1970).
3. A.I. Alikhanian, K.A. Ispirian, A.G. Oganessian and A.G. Tamanian, N.I.M. 89 147 (1970).
4. A.A. Franghian, F.R. Haratjunian, G.A. Hekimian, A.A. Nasarian and G.B. Torgomian, P.L. 34B 227 (1971).
5. G.M. Garibian, Yerevan pre-print EØN-TØ-13 (1970). This article contains references to many other papers on transition radiation.
6. L. Yuan, C.L. Wang and S. Prunster, PRL 23 496 (1969).
7. L. Yuan, C.L. Wang, H. Uto and S. Prunster, PRL 25 1513 (1970).
8. L. Yuan, C.L. Wang, H. Uto and S. Prunster, P.L. 31B 603 (1970).
9. H. Uto, L. Yuan, G. Dell and C.L. Wang, N.I.M. 97 389 (1971)
10. These results were presented in preliminary form at the American Physical Society meeting, Washington, April 1972.
11. R.W. Ellsworth, J. MacFall, P.K. MacKeown and G.B. Yodh, Proceedings of the 6th Inter-American Seminar on Cosmic Radiation La Paz, Bolivia 2 344 (1970).
12. $t_f$ is a function of $\gamma$, the energy and angle of emission of the photon and the foil plasma frequency; for example the value of $t_f$ for emission of 10 keV photons at an angle of $\frac{1}{\gamma}$ ( the peak of the angular distribution) by a particle of $\gamma$ = 6,000 entering mylar is $\sim\frac{1}{4}$ mil.[13].
13. 1 mil. equals $10^{-3}$ inch.
14. S. Parker, R. Jones, J. Kadyk, M.L. Stevenson, T. Katsura, V.Z. Peterson and D. Yount, N.I.M. 97 181 (1971).
15. Although Krypton is radioactive (since atmospheric testing of nuclear bombs introduced fission products) this is not a problem in this experiment since data is taken in coincidence with beam defining counters.
16. J.P. Berge, C.B. Brooks, P.G. Davey, J.F. Harris and J.G. Loken "Proceedings of the Second International Colloquim on PEPR" M.I.T., Cambridge, Mass. May 1970.
17. O. Blunck and S. Leisegang, Zeits. für Phys. 128 500 (1950)
18. G. Knop, A. Minten and B. Nellen, Zeits. für Phys. 165, 533 (1961)
19. Z. Dimcovski, J. Favier, G. Charpak and G. Amato, N.I.M. 94 151 (1971)
20. P.V. Ramana Murthy, N.I.M. 63 77 (1968).
21. The parameter $b^2$, defined by Blunck and Leisegang[17], has the value $\sim$164 for 3 GeV/c $\pi^-$ - mesons crossing a single chamber, and $\sim$15 for a chamber of thickness eleven times this.

22. D. West, Proc. Roy. Soc. A66, 306 (1953)

23. R. Sternheimer and R.F. Peierls, Phys. Rev. B3 3681 (1971)

TABLE 1 IONIZATION ENERGY LOSS

| CHAMBER GAS | MOMENTUM AND PARTICLE | $\gamma$ | MEASURED MOST-PROBABLE ENERGY LOSS PER CHAMBER (SUBJECT TO ~ 20% CALIBRATION UNCERTAINTY) (KeV)* | FULL-WIDTH-HALF-MAXIMUM (KeV)* | RELATIVE MOST-PROBABLE IONIZATION ENERGY-LOSS PER CHAMBER (NORMALISED TO STERNHEIMER-PEIERLS[23] FOR 3 GeV/c $\pi$-MESON) | |
|---|---|---|---|---|---|---|
| | | | | | EXPERIMENT | PREDICTION |
| ARGON | 1.3 GeV/c $\pi^-$ | 9.4 | $1.9 \pm 0.1$ | 2.0 | $1.07 \pm 0.07$ | 1.11 |
| | 3.0 GeV/c $\pi^-$ | 21.6 | $2.2 \pm 0.1$ | 2.1 | 1.24 | 1.24 |
| | 1.3 GeV/c $e^-$ | 2,550 | $2.9 \pm 0.2$ | 2.6 | $1.64 \pm 0.14$ | 1.77 |
| | 3.0 GeV/c $e^-$ | 5,880 | $2.9 \pm 0.2$ | 2.4 | $1.64 \pm 0.14$ | 1.78 |
| KRYPTON | 3.0 GeV/c $\pi^-$ | 21.6 | $4.2 \pm 0.2$ | 3.3 | 1.26 | 1.26 |
| | 3.0 GeV/c $e^-$ | 5,880 | $5.7 \pm 0.3$ | 4.5 | $1.71 \pm 0.13$ | 1.87 |

* See paragraph 2.3; the overall 20% uncertainty in energy calibration is not included in the errors given.

TABLE II TRANSITION RADIATION

| | Momentum Particle | GAS | Radiator | $\gamma$ | 11 Chamber Totals/ Incident Particle (KeV)* | | | |
|---|---|---|---|---|---|---|---|---|
| | | | | | Lower Limit No. of detected Photons | Lower Limit Total Energy Deposition | Ionization Loss Energy Deposition | Lower Limit Transition Radiation Energy Deposition |
| 1 | 3.0 GeV/c $\pi$ | ARGON | 100, ½ mil | 21.6 | 0.3 ± 1 | 36.5 ± 1.8 | 35.2 ± 1.8 | 1.3 ± 2.5 |
| 2 | 1.3 GeV/c $e^-$ | | " | 2,550 | 2.5 ± 0.8 | 57.5 ± 2.8 | 45.0 ± 2.2 | 12.5 ± 3.6 |
| 3 | 3.0 GeV/c $e^-$ | | " | 5,880 | 3.6 ± 0.7 | 70.0 ± 3.5 | 48.6 ± 2.4 | 21.4 ± 4.1 |
| 4. | 1.3 GeV/c $e^-$ | | 100, $\frac{1}{6}$ mil | 2,550 | 1.0 ± 1.0 | 51.6 ± 2.5 | 45.0 ± 2.2 | 6.6 ± 3.3 |
| 5. | 3.0 GeV/c $e^-$ | | " | 5,880 | 2.0 ± 0.8 | 56.6 ± 2.8 | 48.6 ± 2.4 | 8.0 ± 3.7 |
| 6 | 3.0 GeV/c $e^-$ | | 1,50 mil | 5,880 | 0.3 ± 1 | 48.5 ± 2.4 | 47.0 ± 2.3 | 1.5 ± 3.2 |
| 7 | 3.0 GeV/c $e^-$ | | (100, ½ mil (tilted 30° | 5,880 | 3.3 ± 0.7 | 67.6 ± 3.3 | 48.6 ± 2.4 | 19.0 ± 4.1 |
| 8 | 3.0 GeV/c $e^-$ | | 2" styrofoam | 5,880 | 1.4 ± 1 | 57.5 ± 2.8 | 48.6 ± 2.4 | 8.9 ± 3.7 |
| 9 | 3.0 GeV/c $e^-$ | KRYPTON | 100, ½ mil | 5,880 | 5.0 ± 0.5 | 122 ± 6.1 | 85.6 ± 4.2 | 36.4 ± 7.4 |
| 10 | 3.0 GeV/c $e^-$ | | 100, $\frac{1}{6}$ mil | 5,880 | 2.6 ± 0.7 | 100 ± 5.0 | 85.6 ± 4.2 | 14.4 ± 6.5 |

* See paragraph 2.3; there is an overall 20% uncertainty in energy calibration which is not included in the errors given.

## Figure Captions

### Figure 1

Diagram of beam and transition radiation detector.

### Figure 2A

Distribution of ionization energy loss in a single chamber for 3 GeV/c $\pi^-$ - mesons. The curve shows the predictions of Blunck and Leisegang[17]. The chamber thickness is 2.5 $10^{-3}$ gm $cm^{-2}$ and the gas 93% Argon and 7% Methane.

### Figure 2B

Distribution of ionization energy loss for 3 GeV/c $\pi^-$ - mesons when signals from eleven chambers are added. The curve is the Blunck and Leisegang prediction treating the system as one chamber of thickness 27.3 $10^{-3}$ gm $cm^{-2}$ containing 93% Argon and 7% Methane.

### Figure 3A

Distribution of ionization energy loss for 3 GeV/c electrons in single chamber containing 93% Argon and 7% Methane. The curve is the Blunck and Leisegang prediction.

### Figure 3B

Distribution of sum of eleven chambers for ionization loss by 3 GeV/c electrons. The curve is the Blunck and Leisegang prediction treating the system as one chamber of thickness 27.3 $10^{-3}$ gm $cm^{-2}$ containing 93% Argon and 7% Methane.

### Figure 4

Relative most probable energy loss as a function of the ratio momentum/mass. Points marked $^{o}$ are for 93% Argon + 7% Methane, and those marked O are for 93% Krypton + 7% Methane. The curves have been calculated from Sternheimer and Peierls[23]. The relative ionization has been normalised to the calculated values at the points corresponding to the 3 GeV/c $\pi^-$ - meson data (there is no density correction for $\pi^-$ - meson momenta below $\sim$ 14 GeV/c).

### Figure 5A

Distribution of energy deposited in a single Argon/Methane filled chamber when 3 GeV/c electrons pass through the ½ mil. mylar radiators. The points marked with a dot show the distribution obtained <u>without</u> radiators when this is normalized to have equal area in the 1 keV to 3 keV region.

### Figure 5B

As for 5A but for chambers filled with 93% Krypton + 7% Methane. The

dotted distribution has been normalised to equal the histogram area in the 2-5 keV region.

Figure 6

This shows the distributions of total energy deposited in 11 chambers plotted with equal areas for the three cases: 3 GeV/c $\pi^-$ - mesons, 3 GeV/c electrons without radiators, and 3 GeV/c electrons with ½ mil. radiators; chamber gas 93% Argon and 7% Methane. Saturation in some of the readout channels causes a systematic underestimate of the number of large values.

Figure 7

As for Figure 6 but with a gas mixture of 93% Krypton + 7% Methane.

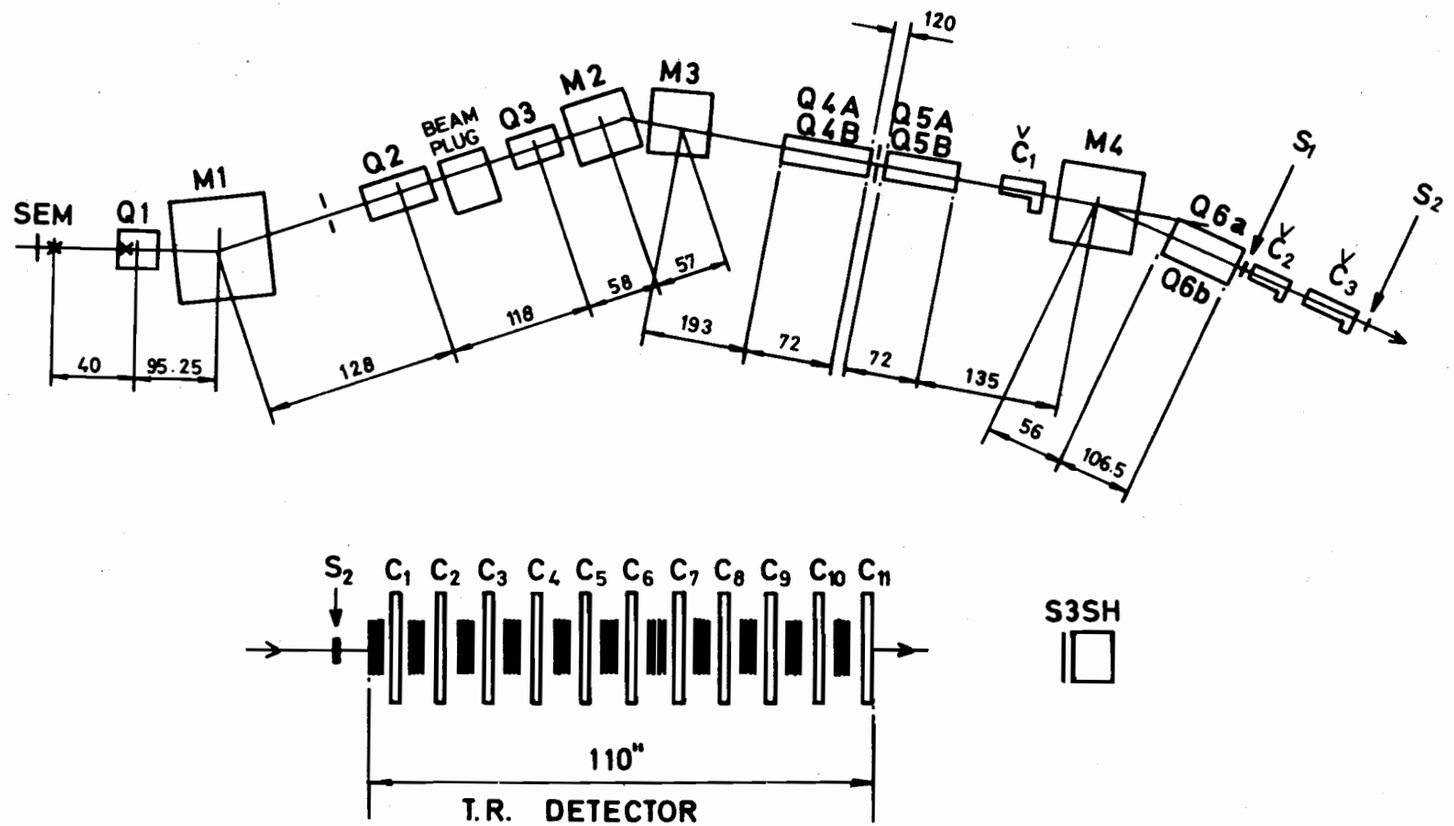
SEM
Q1
M1
Q2
BEAM PLUG
Q3
M2
M3
Q4A
Q4B
Q5A
Q5B
120
C1
M4
Q6a
Q6b
S1
C2
C3
S2
40
95.25
128
118
58
57
193
72
72
135
56
106.5
S2
C1 C2 C3 C4 C5 C6 C7 C8 C9 C10 C11
S3SH
110"
T.R. DETECTOR

Fig. 1

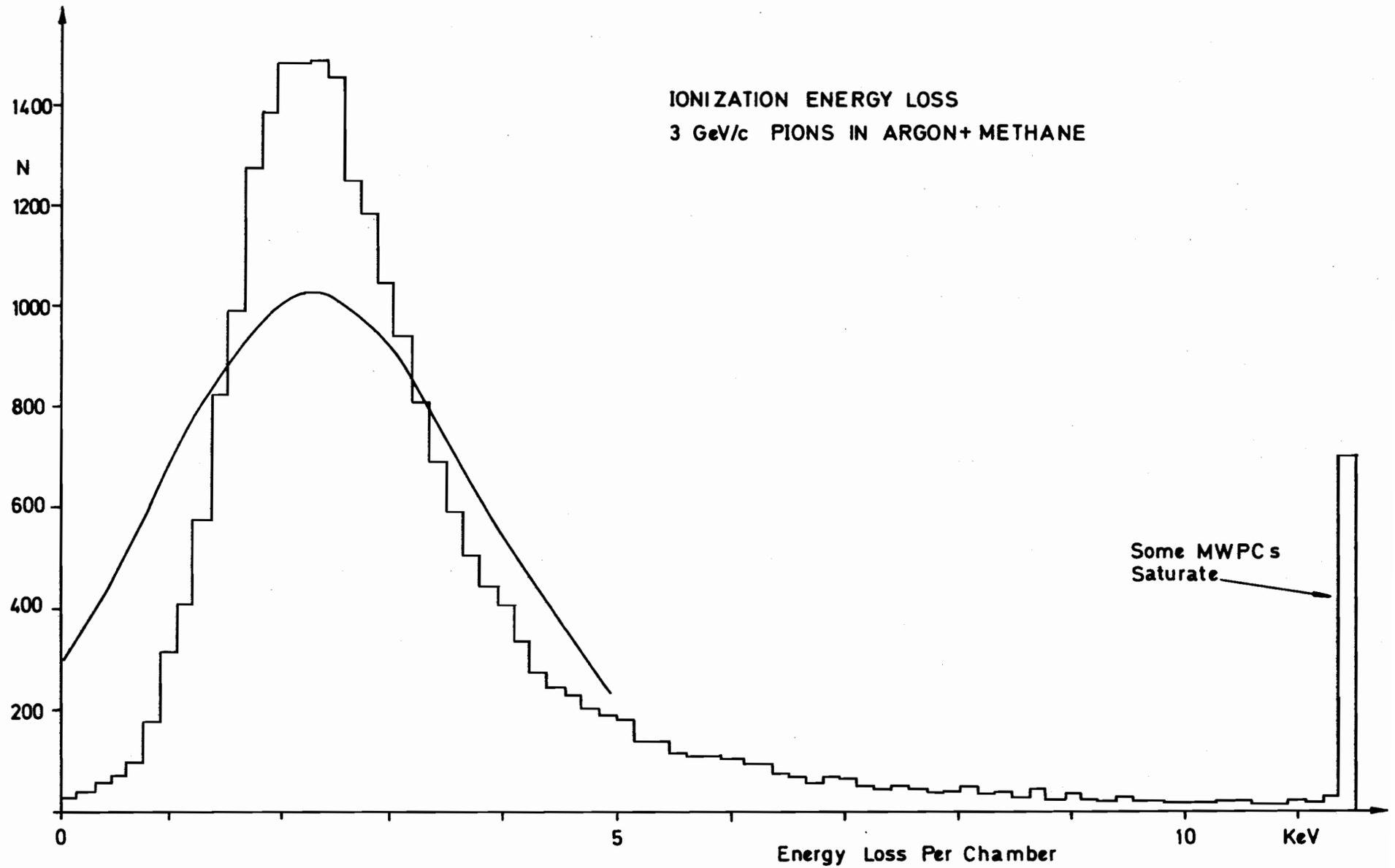
IONIZATION ENERGY LOSS
3 GeV/c PIONS IN ARGON+ METHANE
N
1400
1200
1000
800
600
400
200
0
5
10
KeV
Energy Loss Per Chamber
Some MWPCs
Saturate

Fig. 2A

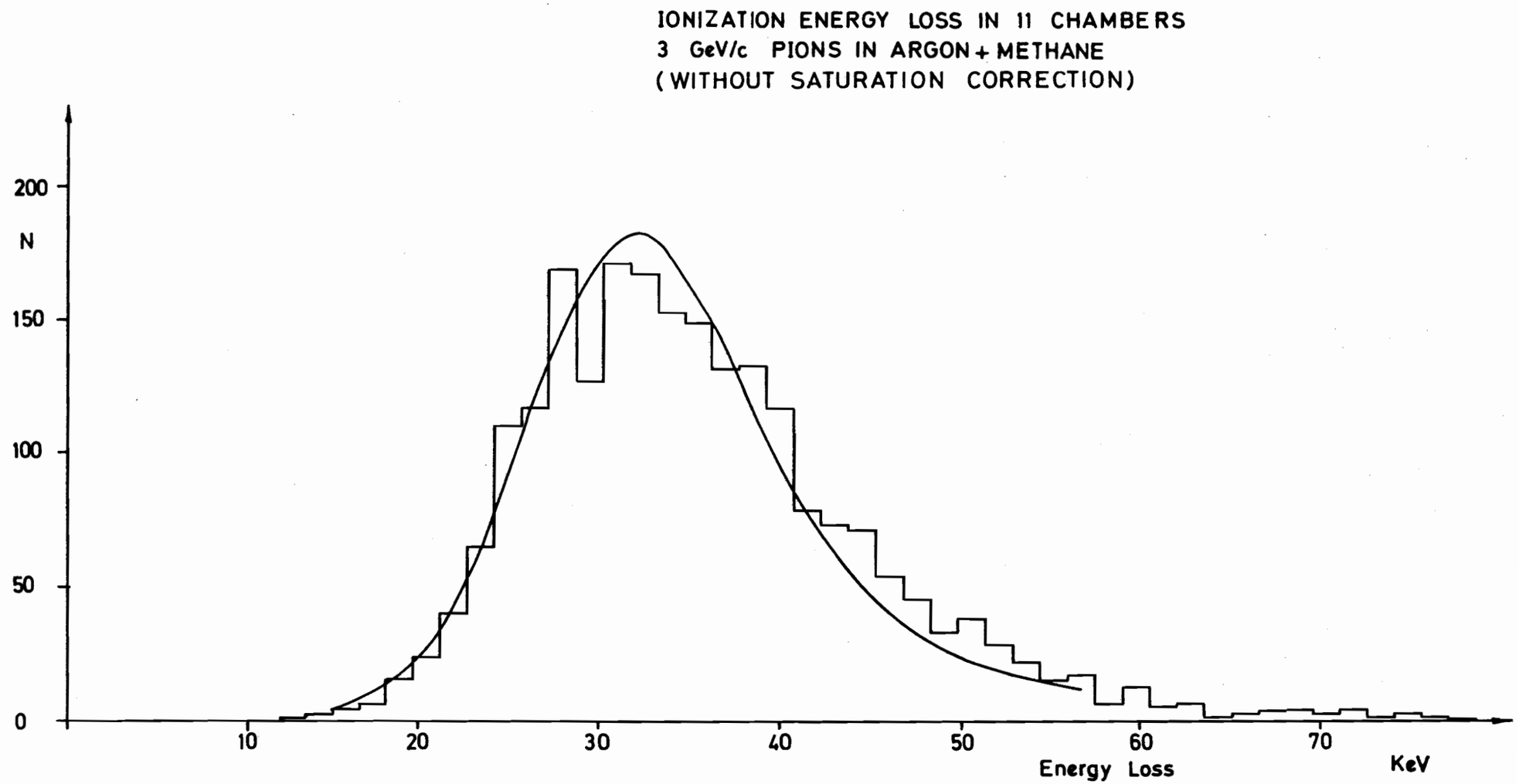
IONIZATION ENERGY LOSS IN 11 CHAMBERS
3 GeV/c PIONS IN ARGON + METHANE
(WITHOUT SATURATION CORRECTION)
200
N
150
100
50
0
10
20
30
40
50
60
70
Energy Loss
KeV

Fig. 2 B

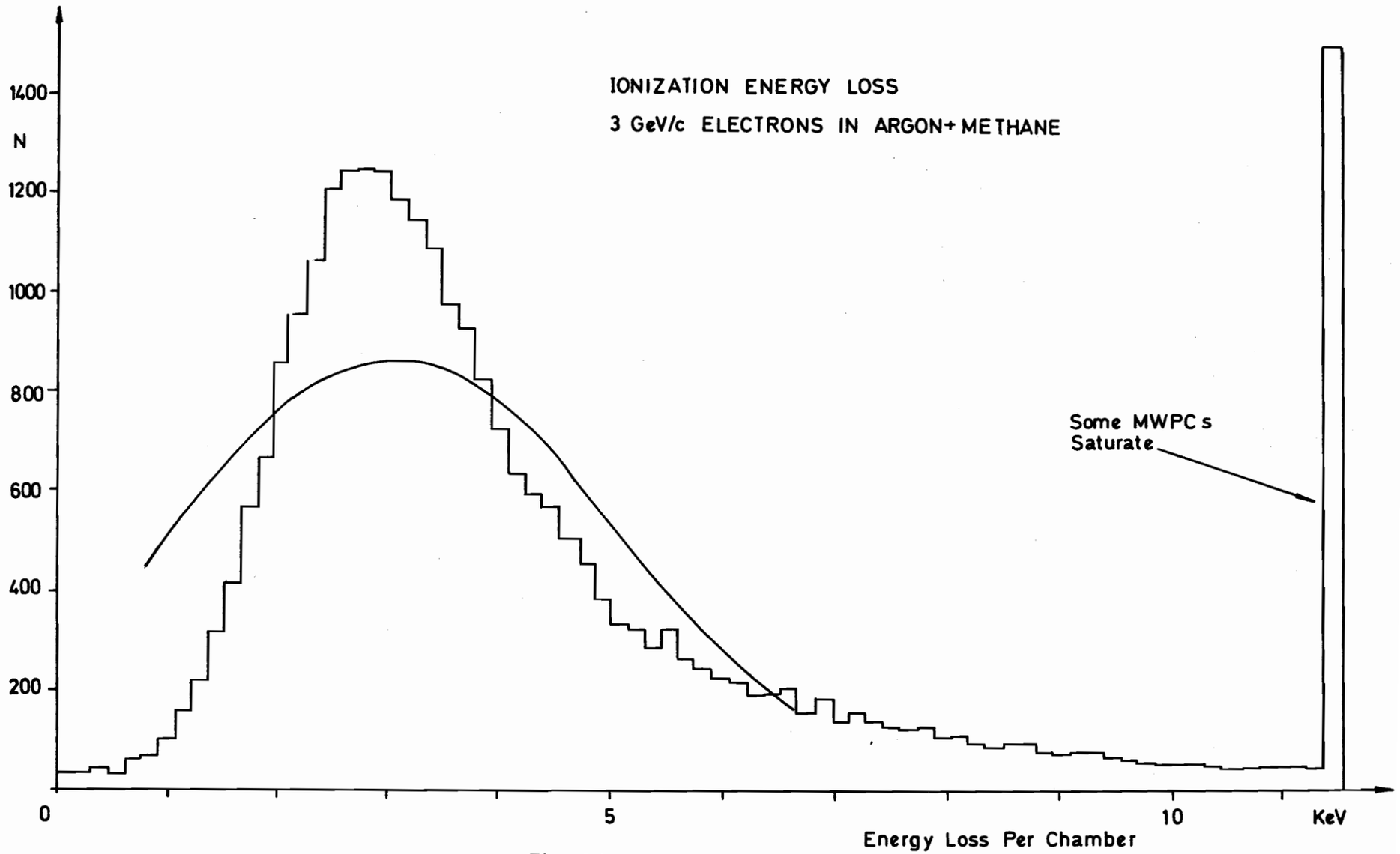
IONIZATION ENERGY LOSS
3 GeV/c ELECTRONS IN ARGON+METHANE
N
1400
1200
1000
800
600
400
200
0
5
10
KeV
Energy Loss Per Chamber
Some MWPC s
Saturate

Fig. 3A

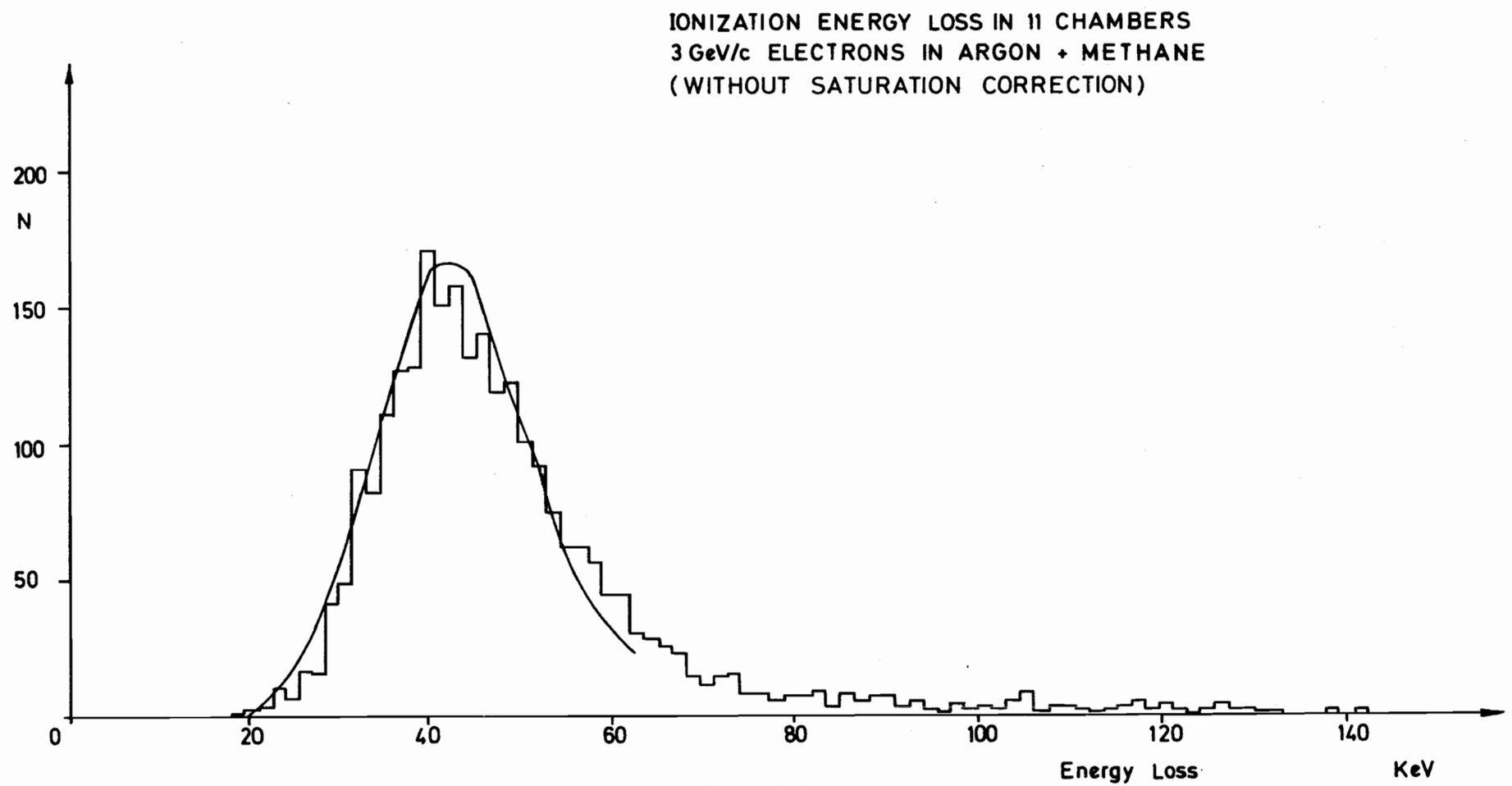
IONIZATION ENERGY LOSS IN 11 CHAMBERS
3 GeV/c ELECTRONS IN ARGON + METHANE
(WITHOUT SATURATION CORRECTION)
200
N
150
100
50
0
20
40
60
80
100
120
140
Energy Loss
KeV

Fig. 3 B

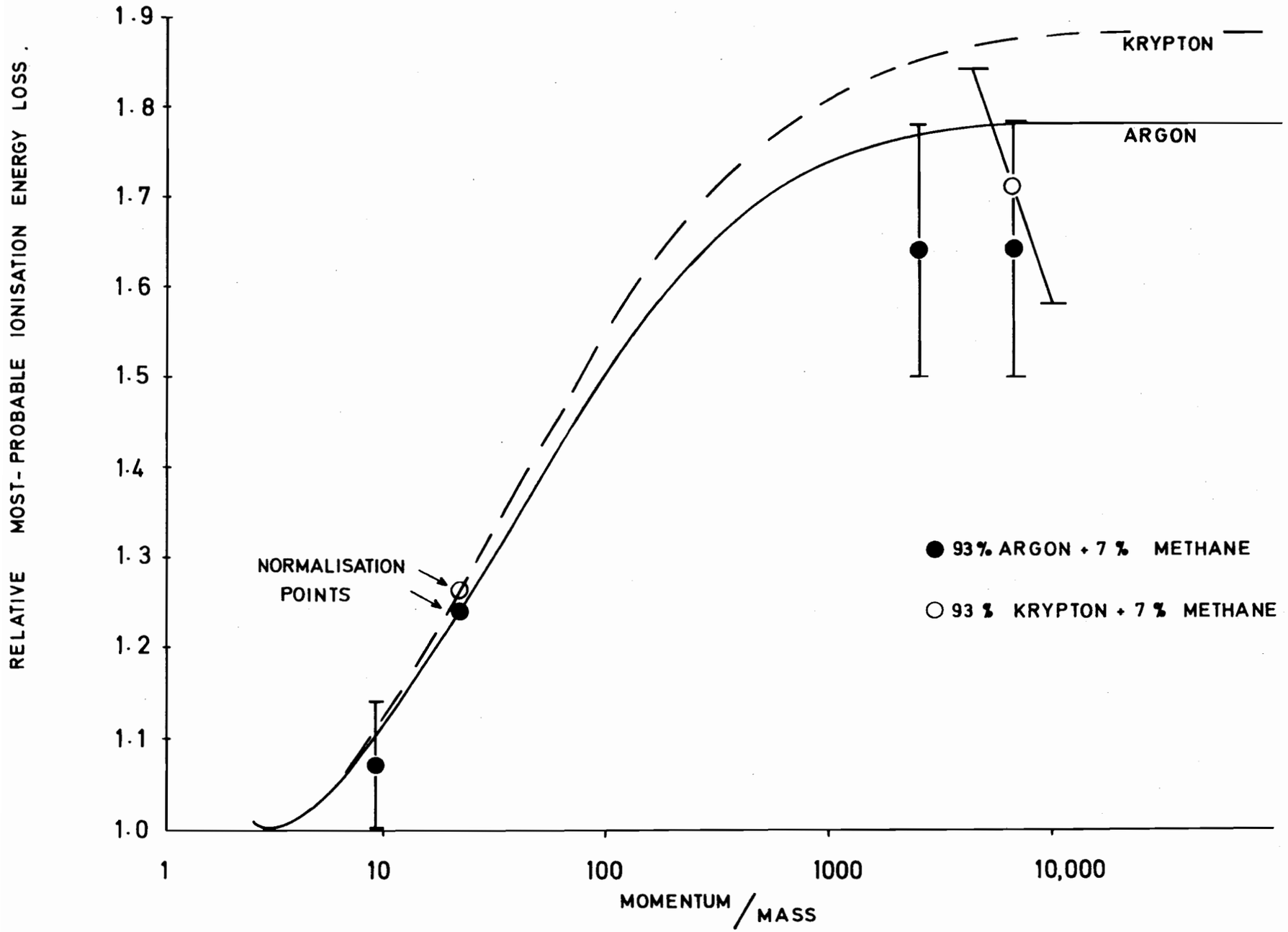
RELATIVE MOST-PROBABLE IONISATION ENERGY LOSS.
1.9
1.8
1.7
1.6
1.5
1.4
1.3
1.2
1.1
1.0
1
10
100
1000
10,000
MOMENTUM / MASS
KRYPTON
ARGON
NORMALISATION POINTS
93% ARGON + 7% METHANE
93% KRYPTON + 7% METHANE

Fig. 4

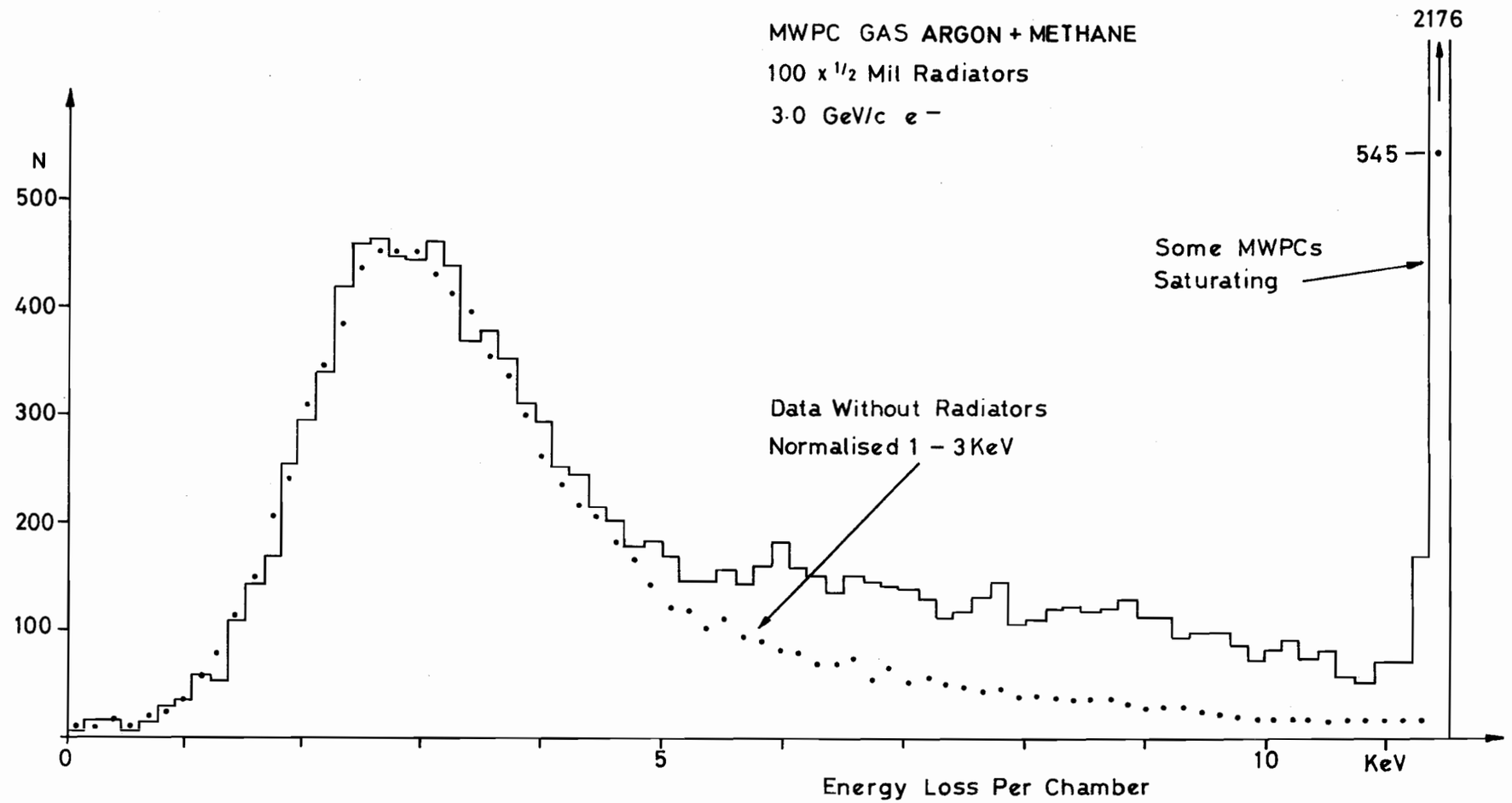
MWPC GAS ARGON + METHANE
100 x 1/2 Mil Radiators
3·0 GeV/c e −
2176
545
N
500
400
300
200
100
Some MWPCs
Saturating
Data Without Radiators
Normalised 1 – 3 KeV
0
5
10
KeV
Energy Loss Per Chamber

Fig. 5 A

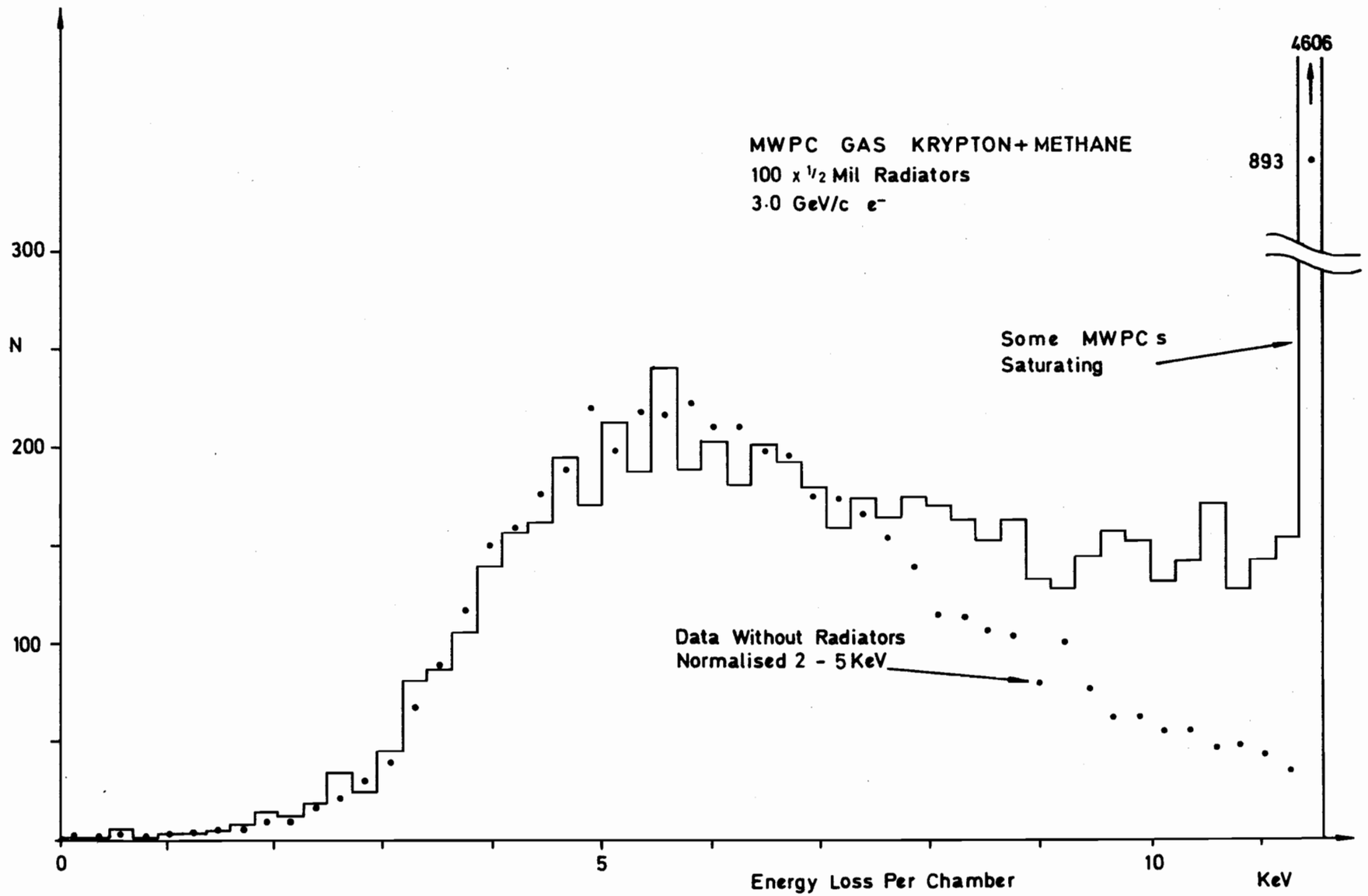
4606
893
MWPC GAS KRYPTON+METHANE
100 x 1/2 Mil Radiators
3.0 GeV/c e⁻
300
N
200
100
Some MWPC s
Saturating
Data Without Radiators
Normalised 2 - 5 KeV
0
5
10
Energy Loss Per Chamber
KeV

Fig. 5 B

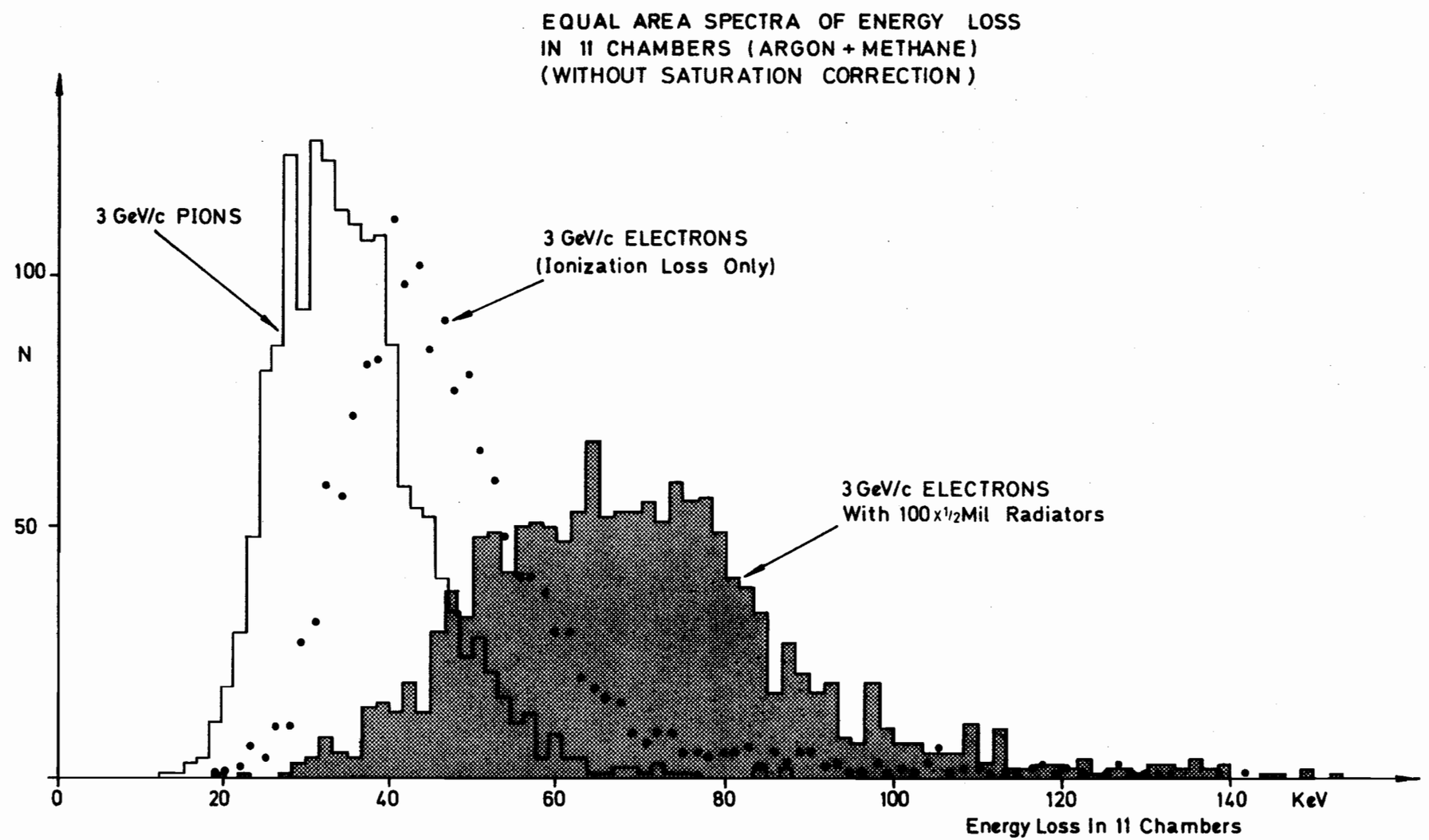
EQUAL AREA SPECTRA OF ENERGY LOSS
IN 11 CHAMBERS (ARGON + METHANE)
(WITHOUT SATURATION CORRECTION)
3 GeV/c PIONS
3 GeV/c ELECTRONS
(Ionization Loss Only)
3 GeV/c ELECTRONS
With 100 x 1/2 Mil Radiators
N
100
50
0
20
40
60
80
100
120
140
KeV
Energy Loss In 11 Chambers

Fig. 6

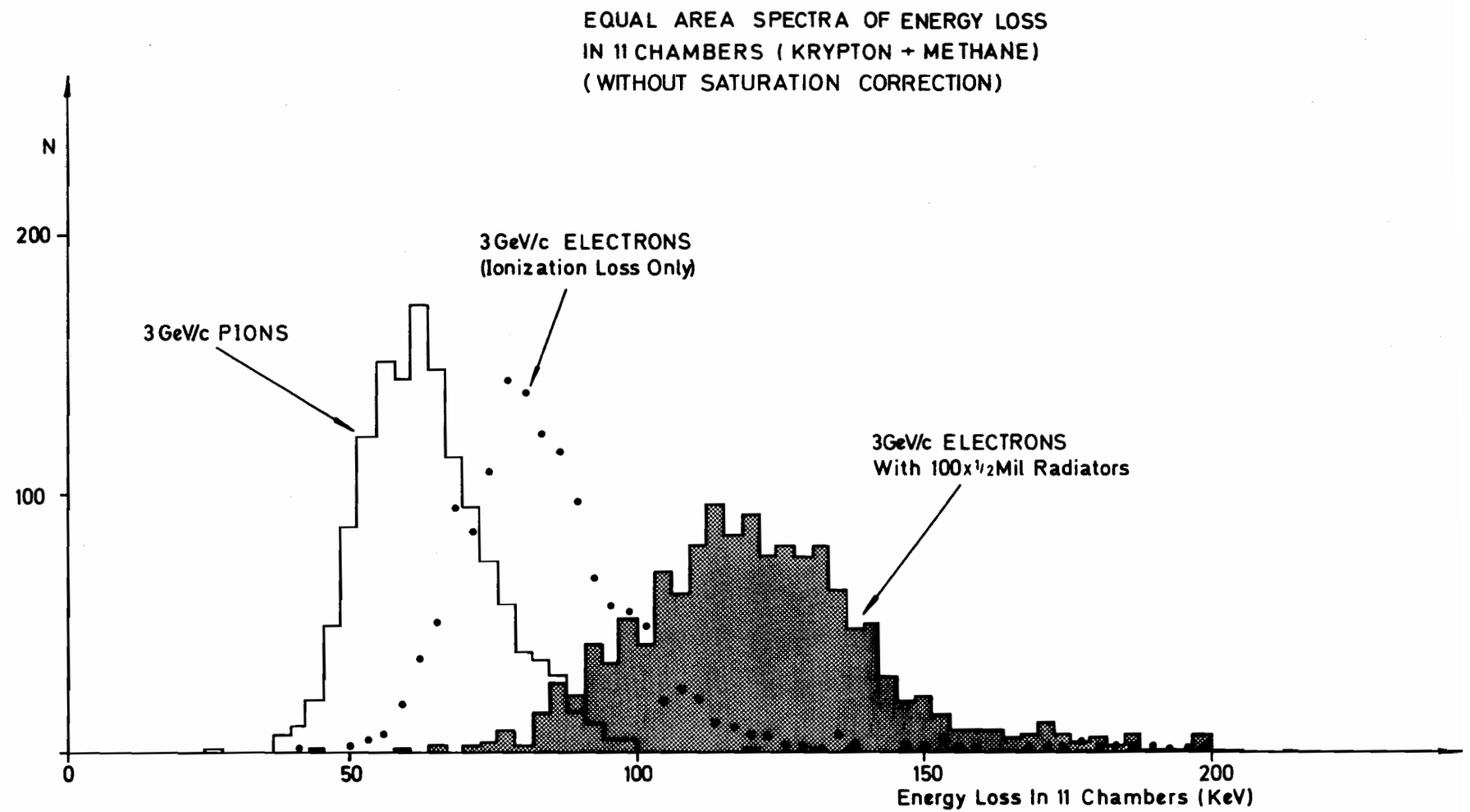
EQUAL AREA SPECTRA OF ENERGY LOSS
IN 11 CHAMBERS ( KRYPTON + METHANE)
( WITHOUT SATURATION CORRECTION)
N
200
100
3 GeV/c ELECTRONS
(Ionization Loss Only)
3 GeV/c PIONS
3GeV/c ELECTRONS
With 100x½Mil Radiators
0
50
100
150
200
Energy Loss In 11 Chambers (KeV)

Fig. 7